References

Al-Bayaty, S., Acharya, D.R., and Hughes, R., Appl. Catal. , 110, pp. 109-119, 1994.

Atchara Saengpoo, Combustion of coke on dehydrogenation catalysts, M.Eng. Thesis, Chulalongkorn University, 1995.

Barbier, J.B., Proceeding of Symposium on Catalyst Deactivation (B. Delmon and G.F. Froment, eds), Studies in Surface Science and Catalysis, Vol.34, pp. 1-10, Elsevier, Amsterdam, 1987.

_____.,J.B., Marecot, N. Martin, L. Elassal, and R. Maurel, Catalyst Deactivation (B. Delmon and G.F.Froment eds), pp. 53, Elsevier, Amsterdam, 1980.

_____., J.B., Corro, G. and Zhang, Y., Appl. Catal., 13, pp. 245-255,1985.

_____., J.B., Corro, G. and Marecot, P., React. Kinet.Catal.Lett., Vol.28, No.2, pp. 245-250 , 1985.

_____., J.B., Appl. Cat., 23, pp. 225-243, 1986.

_____., J.B., Churin, E., and Marecot, P., Appl. Cat., 36, pp. 277-285, 1988.

Barias, O.A., Holmen, A. and Blekkan, E.A., Catalysis Today, 24, pp. 361-364, 1995.

Basso, T.C., Zhang, Z. and Sachtler, W.M.H. , Appl. Cat., 79 , pp. 227-240, 1991.

Beltramini, J. and Trimm, D.L., Appl.Cat., 32, pp. 71-83, 1987.

Biswas, J., Bickle, G.M., Gray, P.G., and Do, D.D., Proceeding of Symposium on Catalyst Deactivation (B. Delmon and G.F. Froment, eds), Studies in Surface Science and Catalysis, Vol.34, Elsevier, Amsterdam, 1987.

Burch, R., and Mitchell, A.J., Appl. Cat. , 6, pp. 121-128, 1983

Butt, John B.and Petersen, Eugene E., Activation, Deactivation and Poisoning of Catalysts, Academic press, Inc.,1988.

Carlos, L., Pieck and Jose'M. Parera, Ind. Eng. Chem. Res., 28, pp. 1785-1788, 1989.

Davis, Mark E. and Suib, Steven L., Selectivity in Catalysis , American Chemical Society, Washington, DC., 1993.

Franck , Jean-Pierre and Martino, Germaine P.,Deactivation of Reforming Catalysts in Jacques Ouder, "Deactivation and Poisoning of Catalysis", Chemical Industries, Vol. 20, Marcel dekker, Inc.,1985.

Fogler , H. Scott, Elements of Chemical Reaction Engineering, 2nd edition, Prentice-Hall , Inc., pp. 625-626, 1992.

Foust, Alan S., Wenzel, Leonard A., Clump, Curtis W., Maus, Louis, and Andersen, L. Bryce, Principles of Unit 2ed Operations, John Wiley&Sons, pp. 703, 1980.

Hughes, R., Deactivation of Catalyst, Academic Press, London, 1984.

Kirszensztejn, P., Foltyniwicz, Z. and Wachowski, L., Ind. Eng. Chem. Res., 30, pp. 2276-2279, 1991.

Levenspiel, O., Chemical Reaction Engineering, 2nd edition, John Wiley & Sons, New York, 1972.

Liwu, L., Tao, Z., Jingling, Z. and Zhusheng, X., Appl. Cat., 67, pp. 11-23, 1990.

Margitfalvi , J., Gobolos, S., Talas, E. Hegedus, M., and Sczedlacsek, P., in B.Delmon and G.F. Froment (eds.), Catalyst Deactivation 1987, pp.147-157 , Amsterdam , Elsevier, 1987.

Parera, J.M., Figoli, N.S., Traffano, E.M., Beltramini, J.N. and Martinelli, E.E., Appl. Cat., 5, pp. 33-41 , 1983.

Pieck, C.L., Jablonski, E.L., Verderone, R.J. and Parera, J.M., Appl. Cat., 56 , pp. 1-8, 1989.

_____., C.L., Jablonski, E.L., and Parera, J.M., Appl.Catal., 70 , pp. 19-28, 1991.

Querini, C.A., and Fung, S.C., Appl. Catal. , 117, pp. 53-74, 1994.

Reid, Robert C., Prausnitz, John M., and Poling, Bruce E., The Properties of Gases & Liquids, McGraw-Hill Book Company, Fourth Edition, 1988.

Satterfield, Charles N., Heterogeneous Catalysts in Practice, McGraw-Hill chemical engineering series, United States of America, 1980.

Smith, J.M., Chemical Engineering Kinetics, McGraw-Hill Book Company, Third Edition, 1981.

Somsak Amornchanthanakorn, Coke formation on dehydrogenation catalysts, M. Eng. Thesis, Chulalongkorn University, 1992.

Tanabe, Kozo, Misono, Makoto, Ono, Yoshio, and Hideshi, Hattori, New Solid Acids and Bases, Studies in Surface Science and Catalysis, Vol.51, pp. 340-341, Elsevier, Amsterdam, 1989.

Tao, Z., Jingling, Z., and Liwu, L., Catalyst Deactivation (C.H. Bartholomew and J.B. Butt, eds), Studies in Surface Science and Catalysis, Vol.34, pp. 143-151 , Elsevier, Amsterdam, 1991.

Wejciechowski, Bohden W. and Corma, Avelino, Catalytic Cracking (Catalysts, Chemistry and Kinetics), Chemical Industries, Volume 25, Marcel dekker, Inc., 1986.

Yining, F., Zhusheng, X., Jingling, Z. and Liwu, L., Catalyst Deactivation (C.H. Bartholomew and J.B. Butt, eds), Studies in Surface Science and Catalysis, Vol.34, pp. 683-690 , Elsevier, Amsterdam, 1991.

APPENDIX A

CALIBRATION CURVE OF CARBON DIOXIDE CONTENT

Table A1 Detected area and estimated weight of carbon by pulsing 100% carbon dioxide through porapak QS column on GC 8AIT at 110°C detector temperature and 90°C column temperature.

Volume (cc.)	Average area (a.u.)	Gas content (mole)	Carbon content (mg)
0.5	501,822	1.83×10^{-5}	0.2198
0.7	754,877	2.57×10^{-5}	0.3078
1.0	1,107,989	3.66×10^{-5}	0.4398
1.2	1,327,272	4.40×10^{-5}	0.5277
1.4	1,576,858	5.13×10^{-5}	0.6157
1.6	1,809,651	5.86×10^{-5}	0.7037

The assumption of gas content calculation was based on the ideal gas law. Therefore, the data fitted with linear equation can be expressed below:

Amount of carbon (mg) , $Y = 4\times10^{-7}$ (Area,X)

where least square error , $R^2 = 0.9979$

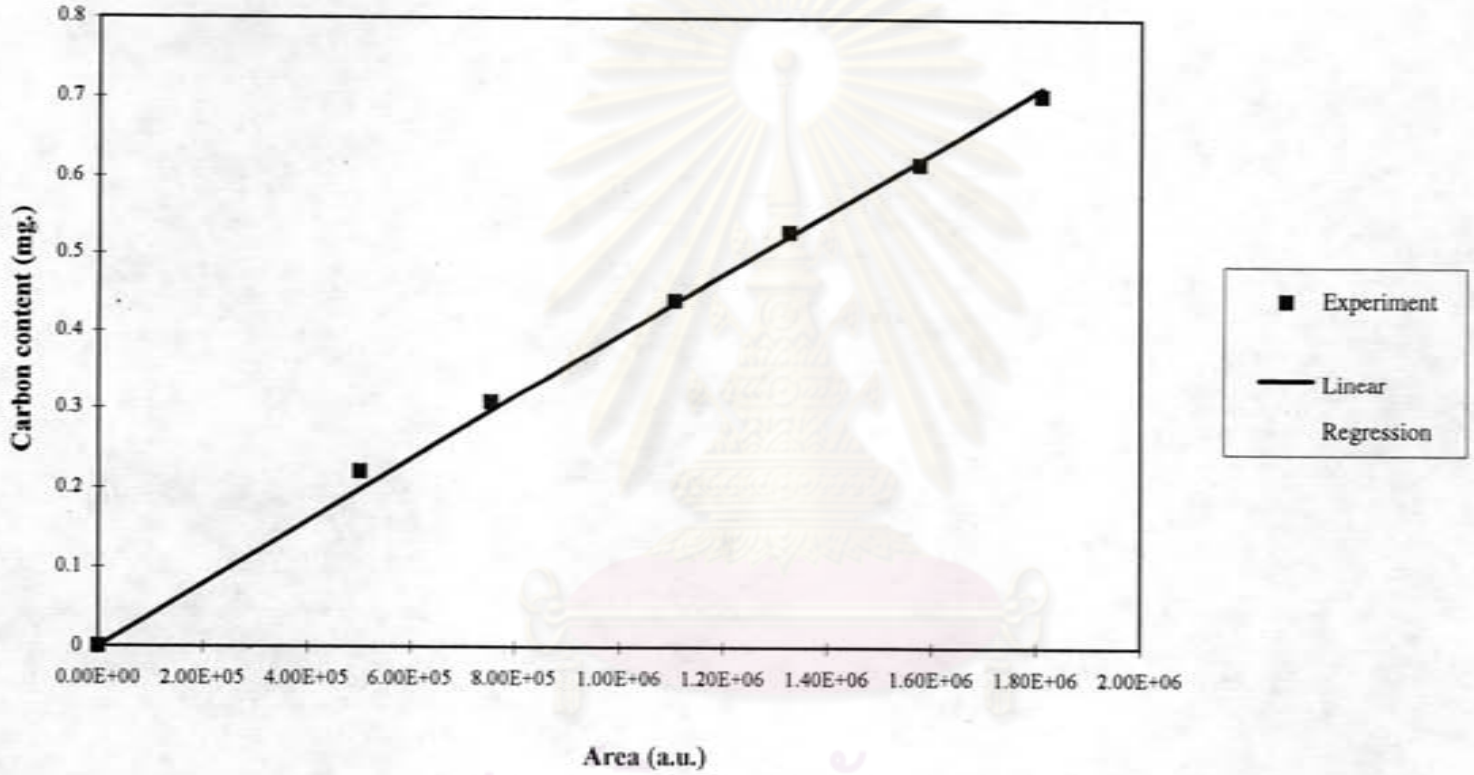

Figure A1 Calibration curve of carbon dioxide on GC 8AIT

APPENDIX B
CALCULATION OF DIFFUSIONAL LIMITATION EFFECT

In the present work there are doubt whether the external and internal diffusion limitations interfere with the propane dehydrogenation reaction and the coke combustion exist. Hence, the kinetic parameters were calculated based on the experimental data so as to prove the controlled system. The calculation is divided into two parts; one of which is the dehydrogenation reaction, and the other is the coke combustion system.

1. Dehydrogenation

The propane dehydrogenation is considered to be an irreversible first-order reaction occurred on the interior pore surface of catalyst particles in a fixed bed reactor. Assume isothermal operation for the reaction.

In the experiment, 20% propane in nitrogen was used as the unique reactant in the system. Molecular weight of nitrogen and propane are 28 and 44, respectively. Thus, the average molecular weight of the gas mixture was calculated as follows:

$$M_{AB} = 0.2\times44 + 0.8\times28$$
$$= 31.2 \text{ g/mol}$$

Calculation of reactant gas density

Consider the propane dehydrogenation is operated at low pressure and high temperature. We assume that the gases are respect to ideal gas law. The density of such gas mixture reactant at various temperatures is calculated in the following.

$$\rho = \frac{PM}{RT} = \frac{1.0 \times 10^5 \times 31.2 \times 10^{-3}}{8.314\ T}$$

We obtained : $\rho = 0.485\ kg/m^3$ at T = 500°C

$\rho = 0.43\ kg/m^3$ at T = 600°C

$\rho = 0.386\ kg/m^3$ at T = 700°C

Calculation of the gas mixture viscosity

The simplified methods for determining the viscosity of low pressure binary mixture are described anywhere (Reid, 1988). The method of Wilke is chosen to estimate the gas mixture viscosity.

For a binary system of 1 and 2,

$$\mu_m = \frac{y_1\mu_1}{y_1 + y_2\phi_{12}} + \frac{y_2\mu_2}{y_2 + y_1\phi_{21}}$$

where μ_m = viscosity of the mixture

μ_1 , μ_2 = pure component viscosity

y_1 , y_2 = mole fractions

$$\phi_{12} = \frac{\left[1 + \left(\frac{\mu_1}{\mu_2}\right)^{1/2}\left(\frac{M_2}{M_1}\right)^{1/4}\right]^2}{\left[8\left(1 + \frac{M_1}{M_2}\right)\right]^{1/2}}$$

$$\phi_{21} = \phi_{12}\left(\frac{\mu_2}{\mu_1}\right)\left(\frac{M_1}{M_2}\right)$$

M_1 , M_2 = molecular weight

Let 1 refer to propane and 2 to nitrogen

$M_1 = 44$ and $M_2 = 28$

From Perry the viscosity of pure nitrogen at 500°C, 600°C and 700°C are 0.036, 0.039 and 0.042 cP, respectively. The viscosity of pure propane at 500°C, 600°C and 700°C are 0.018, 0.021 and 0.023 cP, respectively.

$$\underline{\text{At 500°C}}: \quad \phi_{12} = \frac{\left[1+\left(\frac{0.036}{0.018}\right)^{1/2}\left(\frac{44}{28}\right)^{1/4}\right]^2}{\left[8\left(1+\frac{28}{44}\right)\right]^{1/2}} = 1.844$$

$$\phi_{21} = 1.844\left(\frac{0.018}{0.036}\right)\left(\frac{28}{44}\right) = 0.587$$

$$\mu_m = \frac{0.8\times 0.036}{0.8+0.2\times 1.844}+\frac{0.2\times 0.018}{0.2+0.8\times 0.587} = 0.030 \text{ cP} = 3\times10^{-5} \text{ kg/m-sec}$$

$$\underline{\text{At 600°C}}: \quad \phi_{12} = \frac{\left[1+\left(\frac{0.039}{0.021}\right)^{1/2}\left(\frac{44}{28}\right)^{1/4}\right]^2}{\left[8\left(1+\frac{28}{44}\right)\right]^{1/2}} = 1.763$$

$$\phi_{21} = 1.763\left(\frac{0.021}{0.039}\right)\left(\frac{28}{44}\right) = 0.604$$

$$\mu_m = \frac{0.8\times 0.039}{0.8+0.2\times 1.763}+\frac{0.2\times 0.021}{0.2+0.8\times 0.604} = 0.033 \text{ cP} = 3.3\times10^{-5} \text{ kg/m-sec}$$

$$\underline{\text{At 700°C}}: \quad \phi_{12} = \frac{\left[1+\left(\frac{0.042}{0.023}\right)^{1/2}\left(\frac{44}{28}\right)^{1/4}\right]^2}{\left[8\left(1+\frac{28}{44}\right)\right]^{1/2}} = 1.745$$

$$\phi_{21} = 1.745\left(\frac{0.023}{0.042}\right)\left(\frac{28}{44}\right) = 0.608$$

$$\mu_m = \frac{0.8\times 0.042}{0.8+0.2\times 1.745}+\frac{0.2\times 0.023}{0.2+0.8\times 0.608} = 0.036 \text{ cP} = 3.6\times10^{-5} \text{ kg/m-sec}$$

Calculation of diffusion coefficients

Diffusion coefficients for binary gas system at low pressure calculated by empirical correlation are proposed by Reid (1988). Wilke and Lee method is chosen to estimate the values of D_{AB} due to the general and reliable method. The empirical correlation is

$$D_{AB} = \frac{\left(3.03 - \frac{0.98}{M_{AB}^{1/2}}\right)\left(10^{-3}\right) T^{3/2}}{P\, M_{AB}^{1/2} \sigma_{AB}^{2} \Omega_D}$$

where D_{AB} = binary diffusion coefficient , cm^2/s

T = temperature , K

M_A, M_B = molecular weights of A and B, g/mol

$$M_{AB} = 2\left[\left(\frac{1}{M_A}\right)+\left(\frac{1}{M_B}\right)\right]^{-1}$$

P = pressure, bar

σ = characteristic length , °A

Ω_D = diffusion collision integral, dimensionless

The characteristic Lennard-Jones energy and Length, ε and σ, of nitrogen and propane are as follows : (Reid, 1988)

For N_2 : $\sigma(N_2) = 3.978$ °A , $\varepsilon/k = 71.4$

For C_3H_8 : $\sigma(C_3H_8) = 5.118$ °A , $\varepsilon/k = 237.1$

The simple rules are usually employed.

$$\sigma_{AB} = \frac{\sigma_A + \sigma_B}{2} = \frac{3.798+5.118}{2} = 4.458$$

$$\varepsilon_{AB}/k = \left(\frac{\varepsilon_A \varepsilon_B}{k^2}\right)^{1/2} = (71.4 \times 237.1)^{1/2} = 130.1$$

Ω_D is tabulated as a function of kT/ε for the Lennard-Jones potential. The accurate relation is

$$\Omega_D = \frac{A}{(T^*)^B} + \frac{C}{\exp(DT^*)} + \frac{E}{\exp(FT^*)} + \frac{G}{\exp(HT^*)}$$

where $T^* = \frac{kT}{\varepsilon_{AB}}$, A = 1.06036 , B = 0.15610 , C = 0.19300 , D = 0.47635 , E = 1.03587 , F = 1.52996 , G = 1.76474 , H = 3.89411

Then $T^* = \frac{773}{130.1} = 5.941$ at 500°C

$T^* = \frac{873}{130.1} = 6.710$ at 600°C

$T^* = \frac{973}{130.1} = 7.479$ at 700°C

$$\Omega_D = \frac{1.06036}{(T^*)^{0.15610}} + \frac{0.19300}{\exp(0.47635T^*)} + \frac{1.03587}{\exp(1.52996T^*)} + \frac{1.76474}{\exp(3.89411T^*)}$$

$\Omega_D = 0.814$; 500°C

$\Omega_D = 0.796$; 600°C

$\Omega_D = 0.780$; 700°C

With Equation of D_{AB},

$$\text{At } 500^\circ\text{C} : D(C_3H_8\text{-}N_2) = \frac{\left(3.03 - \frac{0.98}{31.2^{0.5}}\right)(10^{-3})773^{3/2}}{1 \times 31.2^{0.5} \times 4.458^2 \times 0.814} = 0.679 \text{ cm}^2/\text{s}$$

$$= 6.79 \times 10^{-5} \text{ m}^2/\text{s}$$

$$\text{At } 600^\circ\text{C} : D(C_3H_8\text{-}N_2) = \frac{\left(3.03 - \frac{0.98}{31.2^{0.5}}\right)(10^{-3})873^{3/2}}{1 \times 31.2^{0.5} \times 4.458^2 \times 0.796} = 0.833 \text{ cm}^2/\text{s}$$

$$= 8.33 \times 10^{-5} \text{ m}^2/\text{s}$$

$$\text{At } 700^\circ\text{C} : D(C_3H_8\text{-}N_2) = \frac{\left(3.03 - \frac{0.98}{31.2^{0.5}}\right)(10^{-3})973^{3/2}}{1 \times 31.2^{0.5} \times 4.458^2 \times 0.780} = 1.00058 \text{ cm}^2/\text{s}$$

$$= 10.0 \times 10^{-5} \text{ m}^2/\text{s}$$

Reactant gas mixture was supplied at 30 ml/min. in tubular microreactor used in the propane dehydrogenation system at 30°C.

Propane flow rate through reactor = 30 ml/min. at 30°C

The density of propane , $\rho = \frac{1.0\times10^{5}\times31.2\times10^{-3}}{8.314\,(273+30)} = 1.238$ kg/m^3

Mass flow rate $= 1.238\left(\frac{30\times10^{-6}}{60}\right) = 6.19\times10^{-7}$ kg/s

Diameter of quartz tube reactor = 6 mm

Cross-sectional area of tube reactor $= \frac{\pi(6\times10^{-3})^2}{4} = 2.83\times10^{-5}$ m^2

Mass Velocity , $G = \frac{6.19\times10^{-7}}{2.83\times10^{-5}} = 0.022$ kg/m^2-s

Catalyst size = 60-80 mesh = 0.177-0.25 mm

Average catalyst size = (0.25+0.177)/2 = 0.214 mm

Find Reynolds number, Re_p , which is well known as follows:

$$Re_p = \frac{d_p G}{\mu}$$

We obtained

At 500°C : $Re_p = \frac{\left(0.214\times10^{-3}\times0.022\right)}{3\times10^{-5}} = 0.157$

At 600°C : $Re_p = \frac{\left(0.214\times10^{-3}\times0.022\right)}{3.3\times10^{-5}} = 0.143$

At 700°C : $Re_p = \frac{\left(0.214\times10^{-3}\times0.022\right)}{3.6\times10^{-5}} = 0.131$

Average transport coefficients between the bulk stream and particles surface could be correlated in terms of dimensionless groups which characterize the flow conditions. For mass transfer the Sherwood number, $k_m\rho/G$, is an empirical function of the Reynolds number, d_pG/μ , and the Schmidt number, $\mu/\rho\mathcal{D}$. The j-factors are defined as the following functions of the Schmidt and Sherwood numbers:

$$j_D = \frac{k_m \rho}{G}\left(\frac{a_m}{a_t}\right)(\mu/\rho\mathcal{D})^{2/3}$$

The ratio (a_m/a_t) allows for the possibility that the effective mass-transfer area, a_m, may be less than the total external area, a_t, of the particles. For Reynolds number greater than 10, the following relationship between j_D and the Reynolds number well represents available data.

$$j_D = \frac{0.458}{\varepsilon_B}\left(\frac{d_p G}{\mu}\right)^{-0.407}$$

where G = mass velocity(superficial) based upon cross-sectional area of empty reactor

$(G = u\rho)$

d_p = diameter of catalyst particle for spheres

μ = viscosity of fluid

ρ = density of fluid

ε_B = void fraction of the interparticle space (void fraction of the bed)

$\mathcal{D}$ = molecular diffusivity of component being transferred

Assume $\varepsilon_B = 0.5$

At 500°C : $j_D = \frac{0.458}{0.5}(0.157)^{-0.407} = 1.946$

At 600°C : $j_D = \frac{0.458}{0.5}(0.143)^{-0.407} = 2.021$

At 700°C : $j_D = \frac{0.458}{0.5}(0.131)^{-0.407} = 2.095$

A variation of the fixed bed reactor is an essembly of screens or gauze of catalytic solid over which the reacting fluid flows. Data on mass transfer from single screens has been reported by Gay and Maughan (1963). Their correlation is of the form $j_D = \frac{\varepsilon k_m \rho}{G}(\mu/\rho\mathcal{D})^{2/3}$

where ε is the porosity of the single screen.

Hence, $k_m = \left(\frac{j_D G}{\rho}\right)(\mu/\rho\mathcal{D})^{2/3}$

$$k_m = \left(\frac{0.458G}{\varepsilon_B \rho}\right) Re^{-0.407}\, Sc^{-2/3}$$

Find k_m: At 500°C, $k_m = \left(\frac{1.946 \times 0.022}{0.485}\right)(0.911)^{-2/3} = 0.102$ m/s

At 600°C, $k_m = \left(\frac{2.021 \times 0.022}{0.43}\right)(0.921)^{-2/3} = 0.109$ m/s

At 700°C, $k_m = \left(\frac{2.095 \times 0.022}{0.386}\right)(0.932)^{-2/3} = 0.125$ m/s

Find Schmidt number, Sc : $Sc = \frac{\mu}{\rho D}$

At 500°C : $Sc = \frac{3 \times 10^{-5}}{0.485 \times 6.79 \times 10^{-5}} = 0.911$

At 600°C : $Sc = \frac{3.3 \times 10^{-5}}{0.43 \times 8.33 \times 10^{-5}} = 0.921$

At 700°C : $Sc = \frac{3.6 \times 10^{-5}}{0.386 \times 10 \times 10^{-5}} = 0.932$

Properties of catalyst

Density = 3.2 g/ml catalyst

Diameter of 60-80 mesh catalyst particle = 0.214 mm

Weight per catalyst particle $= \frac{\pi(0.214 \times 10^{-1})^3 \times 3.2}{6} = 5.23 \times 10^{-6}$ g/particle

External surface area per particle $= \pi(90.214 \times 10^{-3})^2 = 1.439 \times 10^{-7}$ m^2/particle

$a_m = \frac{1.439 \times 10^{-7}}{5.23 \times 10^{-6}} = 27.51 \times 10^{-3}$ m^2/gram catalyst

Volumetric flow rate of gaseous feed stream = 30 ml/min.

Molar flow rate of gaseous feed stream $= \frac{\left(1 \times 10^5\right)\left(\frac{30 \times 10^{-6}}{60}\right)}{8.314(273+30)} = 1.98 \times 10^{-5}$ mol/s

Propane molar feed rate = $0.2 \times 1.98 \times 10^{-5} = 3.97 \times 10^{-6}$ mol/s

Propane conversion on Pt catalyst (experimental data) = 40%

The estimated rate of propane dehydrogenation reaction is based on the ideal plug-flow reactor which there is no mixing in the direction of flow and complete mixing perpendicular to the direction of flow (i.e., in the radial direction). The rate of reaction will vary with reaction length (W). Plug flow reactors are normally operated at steady state so that properties at any position are constant with respect to time. The mass balance around plug flow reactor becomes

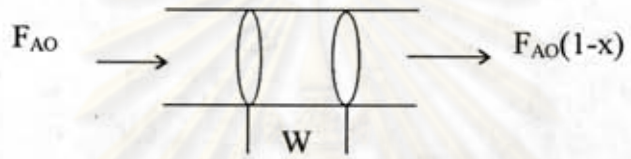

$$\left\{\begin{matrix}\text{rate of i into}\\ \text{volume element}\end{matrix}\right\} - \left\{\begin{matrix}\text{rate of i out of}\\ \text{volume element}\end{matrix}\right\} + \left\{\begin{matrix}\text{rate of production of i within}\\ \text{the volume element}\end{matrix}\right\}$$

$$= \left\{\begin{matrix}\text{rate of accumulation of i within}\\ \text{the volume element}\end{matrix}\right\}$$

$F_{AO} = F_{AO}(1-x) + (r_w W)$

$(r_w W) = F_{AO} - F_{AO}(1-x) = F_{AO}\, x$

$$r_w = \frac{F_{AO} x}{W} = \frac{3.97 \times 10^{-6} \times 0.4}{0.1} = 1.588 \times 10^{-5} \quad \text{mol/s-gram catalyst}$$

At steady state the external transport rate may be written in terms of the diffusion rate from the bulk gas to the surface. The expression is:

$$r_{obs} = k_m\, a_m\, (C_b - C_s)$$

$$= \frac{\text{Propane conversion (mole)}}{\text{(time) (gram of catalyst)}}$$

where C_b and C_s are the concentrations in the bulk gas and at the surface, respectively.

At 600°C, $(C_b - C_s) = \dfrac{r_{obs}}{k_m a_m} = \dfrac{1.588 \times 10^{-5}}{0.109 \times 27.5 \times 10^{-3}} = 5.3 \times 10^{-3}$ mol/m^3

From C_b (propane) = 2.76 mol/m^3

Consider the difference of the bulk and surface concentration is small value. It means that the external mass transport has no effect on the dehydrogenation reaction rate.

Next, consider the internal diffusional limitation of the dehydrogenation reaction. An effectiveness factor, η, was defined in order to express the rate of reaction for the whole catalyst pellet, r_p, in terms of the temperature and concentrations existing at the outer surface (Smith, 1981) as follows:

$$\eta = \frac{\text{actual rate of the whole pellet}}{\text{rate evaluated at outer surface conditions}} = \frac{r_p}{r_s}$$

The equation for the local rate (per unit mass of catalyst) may be expressed functionally as $r = f(C,T)$, where C represents, symbolically, the concentrations of all the involved components. Then

$$r_p = \eta r_s = \eta f(C_s, T_s)$$

Suppose that the propane dehydrogenation is an irreversible reaction $A \rightarrow B$ and first order reaction, so that for isothermal conditions $r = f(C_A) = k_1 C_A$.
Then $r_p = \eta k_1 (C_A)_s$

For a spherical pellet, a mass balance over the spherical-shell volume of thickness Δr. At steady state the rate of diffusion into the element less the rate of diffusion out will equal the rate of disappearance of reactant within the element. This rate will be $\rho_p k_1 C_A$ per unit volume, where ρ_p is the density of the pellet. Hence, the balance may be written, omitting subscript A on C,

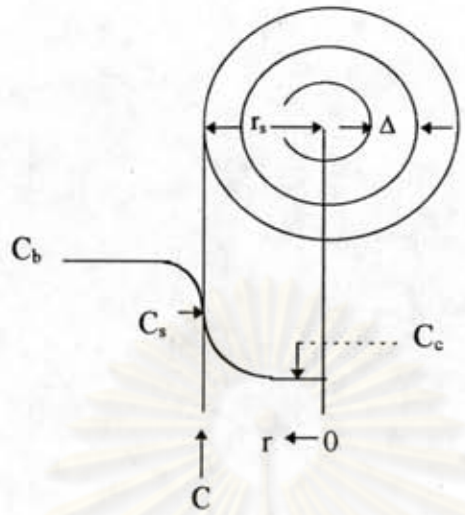

Figure B1 Reactant (A) concentration vs. position for first-order reaction on a spherical catalyst pellet.

$$\left(-4\pi r^2 D_e \frac{dC}{dr}\right)_r - \left(-4\pi r^2 D_e \frac{dC}{dr}\right)_{r+\Delta r} = 4\pi r^2 \Delta r \rho_p k_1 C$$

Take the limit as $\Delta r \rightarrow 0$ and assume that the effective diffusivity is independent of the concentration of reactant, this difference equation becomes

$$\frac{d^2C}{dr^2} + \frac{2dC}{rdr} - \frac{k_1 \rho_p C}{D_e} = 0$$

At the center of the pellet symmetry requires

$$\frac{dC}{dr} = 0 \text{ at } r = 0$$

and at the outer surface

$$C = C_s \text{ at } r = r_s$$

Solve linear differential equation by conventional methods to yield

$$\frac{C}{C_s} = \frac{r_s \sinh(3\phi_s \frac{r}{r_s})}{r \sinh 3\phi_s}$$

where ϕ_s is Thiele modulus for a spherical pellet defined by $\phi_s = \frac{r_s}{3}\sqrt{\frac{k_1 \rho_p}{D_e}}$

Both D_e and k_1 are necessary to use $r_p = \eta k_1 (C_A)_s$. D_e could be obtained from the reduced pore volume equation in case of no tortuosity factor.

$$D_e = (\varepsilon_s^2 D_{AB})$$

At 500°C , $D_e = (0.5)^2 (6.79\times10^{-5}) = 1.7\times10^{-5}$

At 600°C , $D_e = (0.5)^2 (8.33\times10^{-5}) = 2.08\times10^{-5}$

At 700°C , $D_e = (0.5)^2 (10\times10^{-5}) = 2.5\times10^{-5}$

Substitute radius of catalyst pellet , $r_s = 0.107\times10^{-3}$ m with ϕ_s equation

$$\phi_S = \frac{0.107\times10^{-3}\,m}{3}\sqrt{\frac{k(m^3/s-kg\ cat.)\times3200(kg/m^3)}{2.08\times10^{-5}(m^2/s)}}\text{, at 600°C}$$

$$\phi_S = 0.442\sqrt{k} \qquad \text{(dimensionless)}$$

Find k from the mass balance equation around plug-flow reactor.

$$r_w = \frac{F_{Ao}dx}{dW}$$

where $r_w = kC_A$

Thus, $kC_A = \frac{F_{Ao}dx}{dW}$

$$k\,C_{Ao}(1\text{-}x) = \frac{F_{Ao}dx}{dW}$$

$$W = \frac{F_{Ao}}{kC_{Ao}}\int_0^{0.4}\frac{1}{1-x}dx$$

$$W = \frac{F_{Ao}}{kC_{Ao}}[-\ln(1-x)]_0^{0.4} = \frac{F_{Ao}}{kC_{Ao}}(-\ln(0.6))$$

$$k = \frac{F_{Ao}}{WC_{Ao}}(-\ln(0.6))$$

$$k = \frac{3.97\times10^{-6}(mol/s)}{0.1\times10^{-3}(kg)\times2.76(mol/m^3)}(-\ln(0.6)) = 0.00735\ m^3/s\text{- kg catalyst}$$

Calculate ϕ_s : $\phi_S = 0.442\sqrt{0.00735} = 0.0379$

For such small values of ϕ_s it was concluded that the internal mass transport has no effect on the rate of dehydrogenation reaction. Therefore, Coke could be formed on the surface of pores.

2. Coke Combustion

1 % O_2 in He was used as an oxidizing reagent in the coke combustion system. Molecular weight of helium and oxygen are 4.003 and 31.999, respectively. Then, the average molecular weight of gas mixture is

$$M_{AB} = 0.01\times31.999 + 0.99\times4.003 = 4.283 \text{ g/mol}$$

For He : $\sigma(He) = 2.551\ ^{\circ}A$, $\varepsilon/k = 10.22$ K

For O_2 : $\sigma(O_2) = 3.467\ ^{\circ}A$, $\varepsilon/k = 106.7$ K

The simple rules are usually employed.

$$\sigma_{AB} = \frac{\sigma_A + \sigma_B}{2} = \frac{2.551+3.467}{2} = 3.009\ ^{\circ}A$$

$$\varepsilon_{AB}/k = \left(\frac{\varepsilon_A \varepsilon_B}{k^2}\right)^{1/2} = (10.22\times106.7)^{1/2} = 33.02$$

Ω_D is tabulated as a function of kT/ε for the Lennard-Jones potential. The accurate relation is

$$\Omega_D = \frac{A}{(T^*)^B} + \frac{C}{\exp(DT^*)} + \frac{E}{\exp(FT^*)} + \frac{G}{\exp(HT^*)}$$

where $T^* = \frac{kT}{\varepsilon_{AB}}$, A = 1.06036 , B = 0.15610 , C = 0.19300 , D = 0.47635 ,

E = 1.03587 , F = 1.52996 , G = 1.76474 , H = 3.89411

Then $T^* = \frac{773}{33.02} = 23.41$ at 500°C

$$T^* = \frac{873}{33.02} = 26.438 \text{ at } 600^{\circ}C$$

$$T^* = \frac{973}{33.02} = 29.467 \text{ at } 700^{\circ}C$$

$$\Omega_D = \frac{1.06036}{(T^*)^{0.15610}} + \frac{0.19300}{\exp(0.47635T^*)} + \frac{1.03587}{\exp(1.52996T^*)} + \frac{1.76474}{\exp(3.89411T^*)}$$

$\Omega_D = 0.648$; 500°C

$\Omega_D = 0.636$; 600°C

$\Omega_D = 0.625$; 700°C

With Equation of D_{AB},

$$\text{At } 500^\circ\text{C} : D(O_2\text{-He}) = \frac{\left(3.03 - \frac{0.98}{4.283^{0.5}}\right)(10^{-3})773^{3/2}}{1 \times 4.283^{0.5} \times 3.009^2 \times 0.648} = 4.525 \text{ cm}^2/\text{s}$$

$$= 4.525 \times 10^{-4} \text{ m}^2/\text{s}$$

$$\text{At } 600^\circ\text{C} : D(O_2\text{-He}) = \frac{\left(3.03 - \frac{0.98}{4.283^{0.5}}\right)(10^{-3})873^{3/2}}{1 \times 4.283^{0.5} \times 3.009^2 \times 0.636} = 4.610 \text{ cm}^2/\text{s}$$

$$= 4.610 \times 10^{-4} \text{ m}^2/\text{s}$$

$$\text{At } 700^\circ\text{C} : D(O_2\text{-He}) = \frac{\left(3.03 - \frac{0.98}{4.283^{0.5}}\right)(10^{-3})973^{3/2}}{1 \times 4.283^{0.5} \times 3.009^2 \times 0.625} = 4.692 \text{ cm}^2/\text{s}$$

$$= 4.692 \times 10^{-4} \text{ m}^2/\text{s}$$

Gas mixture of Oxygen was supplied at flow rate of 30 ml/min. and 30 °C

Therefore, molar flow rate of the gas mixture is

$$\text{Molar flow rate} = \frac{(1 \times 10^5)(\frac{30 \times 10^{-6}}{60})}{8.314(273+30)} = 1.98 \times 10^{-5} \text{ mol/s}$$

Oxygen molar feed rate = $0.01 \times 1.98 \times 10^{-5}$ mol/s = 1.98×10^{-7} mol/s

Calculate the concentration of oxygen by assuming the ideal gas properties :

$PV = nRT$

The total concentration of gas mixture : $C = \frac{P}{RT} = \frac{1.0 \times 10^5}{8.314(500+273)} = 15.56$ mol/l

The concentration of oxygen component : $C_s = 0.01 \times 15.56 = 0.1556$ mol/l

$= 4.9792$ gram/l

$= 4.9792 \times 10^{-9}$ kg /m^3

Refer to the experimental data from TGA which shown the weight of coke burning on Pt catalyst : Weight of regenerated catalyst = 11.56 mg

Weight of coke = 0.711 mg = 6.15%

Observe the rate of coke combustion based on TGA data:

T = 506.1 °C , Sample weight = 11.74 mg, time = 96.5 minutes

and T = 496 °C , Sample weight = 11.76 mg, time = 94.50 minutes

Then, $r_{obs} = \frac{(11.76 - 11.74)\text{mg coke}}{(2\,\text{min})(11.56\,\text{mg catalyst})} = 8.65 \times 10^{-4}$ kg coke/min.-kg catalyst

or $r_{obs} = 1.442 \times 10^{-5}$ kg coke/s-kg catalyst

The density of catalyst particle , $\rho_p = 3.2$ g/ml $= 3.2 \times 10^{-6}$ kg /m^3

Check the criteria for the importance of internal diffusional limitations on coke combustion reaction . With Weisz-Prater criterion (1954) ,

For the first-order reaction ,

$$\phi = \frac{V}{S}\sqrt{\frac{k\rho_p}{De_A}}$$

Using the values of $k\rho_s = \frac{\phi^2}{L^2} De_A$ with $r_s\rho_s = \eta k \rho_s C_s^s$ gives $r_s\rho_s = \eta \frac{\phi^2}{L^2} De_A C_s^s$

$$\frac{(r_A\rho_s)_{obs} L^2}{De_A C_s^s} = \eta\phi^2$$

1. For $\phi << 1$, $\eta = 1$ (no pore diffusion limitation)

2. For $\phi >> 1$, $\eta = 1/\phi$ that is strong pore diffusion limitation .

$$\frac{r_{obs}\rho_p L^2}{De_A C_s} = \frac{1.442\times10^{-5}\,\frac{\text{kg coke}}{\text{s-kg cat.}} \times 3.2\times10^{-6}\,\frac{\text{kg cat.}}{\text{m}^3} \times \left(\frac{0.107\times10^{-3}}{3}\right)^2 \text{m}^2}{1.62\times10^{-5}(\text{m}^2/\text{s}) \times 4.9792\times10^{-9}(\text{kg/m}^3)}$$

$= 7.277 \times 10^{-7}$ (dimensionless)

Regarding of the small values of ϕ , it clearly shown that the coke combustion system occurred without the significant internal diffusional limitations.

APPENDIX C

Pt-Sn/Al_2O_3 CATALYSTS

Platinum and tin present a complex situation since a number of alloy compositions are possible, depending upon the Sn/Pt ratio. The phase diagram in figure C1 shows that as the Sn/Pt ratio increases it should be possible to form a series of alloys with increasing Sn fractions.

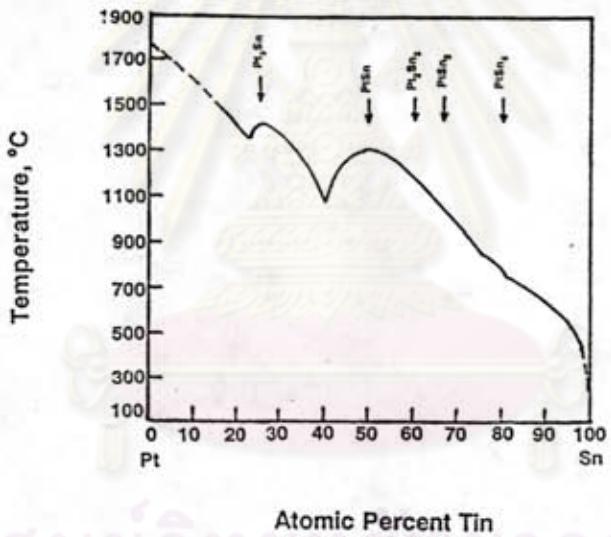

Figure C1 Phase diagram of platinum-tin.

The summary of some catalyst characterization data were established by Davis (1994) from methods that make a more direct measure of the chemical or physical state of the Pt and/or Sn present in Pt-Sn-alumina catalysts. They are as follows:

Temperature-programmed reduction (TPR), one of the indirect analysis methods, yielded data that suggested that Sn was not reduced to zero-valent state. Lieske and Volter (1984) reported, based on the results obtained from TPR studies, that a minor part of tin was reduced to the metal, and this Sn(0) combined with Pt to

form "alloy clusters" but the major portion of the tin was reduced to only Sn(II) state. They also reported that the amount of alloyed tin increased with increasing tin content.

X-ray photoelectron spectroscopy (XPS) studies permit one to determine the chemical state of an element but the data does not permit one to define whether Sn(0), if present, is in the form of a Pt-Sn alloy. Furthermore, the major Pt XPS peak coincides with a large peak from the alumina support. Thus, XPS can only provide to indicate whether an alloy is possible; it cannot be used to prove the presence of a Pt-Sn alloy.

Davis has indicated that the tin is present only in an oxidized state from the XPS studies. Furthermore, Li et.al.(1988) reported that a portion of the tin in Pt-Sn-alumina catalysts was present in the zero valence state; it additionally appears that the composition of the Pt-Sn alloy, based upon the amount of Pt in the catalyst and the Sn (0) detected by XPS, increases with increasing ratios of Sn/Pt.

He described the tin Mössbauer data that it also provides a bulk diagnostic and this method has been utilized in a number of studies. Direct evidence for PtSn alloy formation was obtained from Mössbauer studies; however, many of these studies were at high metal loading and even then a complex spectrum was obtained so that there was some uncertainty in assigning Sn(0) to the exclusion of tin oxide phases.

Li et.al. (1991) utilized the same series of catalysts that had been utilized earlier in their XPS studies; each sample in the three series contained 1 wt.% Pt and a varying amount of Sn. Tin was observed in forms whose isomer shifts were the same as SnO_2, SnO, $SnCl_4$, $SnCl_2$, Sn(0) and PtSn alloy when alumina was the support. If it is assumed that the Pt/Sn alloy corresponds only to PtSn alloy as was found to be the case in X-ray diffraction (XRD) data to be described below, one obtains the results shown in Figure C2. For lower Sn:Pt ratios (5 or less) little difference is observed in the extent of alloy formation and the distribution of the oxidized species for a low and

high surface area alumina support. In this respect, there is general agreement with data observed in some of the earlier Mössbauer studies.The Mössbauer data in Figure C2 show a similar trend in the extent of alloy formation for the alumina supported materials; the fraction of Pt present in an alloy phase increases with increasing tin concentration and only approaches complete alloy formation at Sn:Pt > *ca*.5.

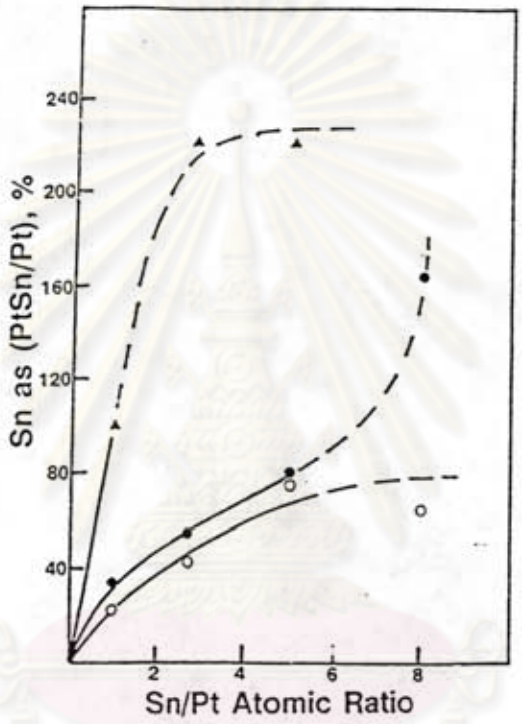

Figure C2 Amount of tin calculated to be present as PtSn alloy versus tin:Pt ratio: Δ silica support, ● low surface area alumina support, ○ high surface area alumina support.

For Pt supported on a co-precipitated tin oxide-alumina catalyst, alloy formation occurs to a much smaller extent than it does on a material prepared by impregnation with the chloride complex of the two metals. Since most commercial catalyst formulations are based on tin-alumina co-precipitated support materials, it appears that the studies using Pt and Sn co-impregnation techniques, while interesting, are not directly applicable to the commercial catalysts.

A catalyst prepared by impregnating a Degussa Aluminum Oxide C (a nonporous alumina with a surface area of 110 m^2/g) with an acetone solution of $Pt_3(SnCl_3)_{20}^{2-}$ was characterized by X-ray Diffraction (XRD). A sample of a catalyst containing 5 wt.% Pt was reduced *in situ* in the chamber of an XRD instrument; thus the material was not exposed to the atmosphere prior to recording the X-ray diffraction pattern. The X-ray diffraction patterns match very well, both in position and intensity, the pattern reported for PtSn alloy. With the 5 wt.% Pt catalyst, a small fraction of the Pt is present as crystalline Pt but crystalline Pt was not observed for the 0.6 wt.% Pt catalyst. It is noted that similar results for the PtSn alloy are obtained for a catalyst that contains only 0.6 wt.% Pt, and with the same Sn/Pt ratio as the 5% Pt catalyst. These *in situ* XRD studies therefore support alloy formation with a stoichiometry of Pt:Sn = 1:1. The Sn in excess of that needed to form this alloy is present in an X-ray "amorphous" form, and is postulated to be present in a shell layer with a structure similar to tin aluminate. A series of catalysts were prepared to contain 1 wt.% Pt and Sn:Pt ratios ranging from *ca*. 1 to 8 using a low (110 m^2/g) and high (300 m^2/g) surface area alumina. XRD studies indicated that, irrespective of the Sn/Pt ratio, the only crystalline phase detected by XRD was PtSn (1:1). The XRD intensity of lines for the SnPt alloy phase increase with increasing Sn:Pt ratios, indicating the presence of unalloyed Pt in the samples containing low tin loading.

Li et.al. (1989) obtained X-ray absorption near edge structure (XANES) and extended X-ray absorption fine structure spectra (EXAFS) for a series of Sn/Pt on alumina or silica samples. The data suggested the possibility of Pt/Sn alloy formation, but did not provide conclusive proof for this.

An electron microdiffraction technique was employed to identify crystal structures developed in two Pt-Sn-alumina catalysts. One catalyst was prepared by co-precipitating Sn and Al oxides and then impregnating the calcined material with chloroplatinic acid to give a Pt:Sn = 1:3 atomic ratio. The second catalyst was prepared by co-impregnating Degussa alumina with an acetone solution of

chloroplatinic acid and stannic chloride to provide a Pt:Sn = 1:3. Pt-Sn alloy was not detected by X-ray diffraction for the co-precipitated catalyst although evidence for PtSn alloy was found for the co-impregnated catalyst.

Pt-Sn-Alumina Structure (Davis, 1994)

No single model will adequately describe the above catalyst characterization data and the published data that has not been included because of space limitations. The relative distribution of both the Pt and Sn species depend upon a number of factors such as surface area of the support, calcination and/or reduction temperature, Sn/Pt ratio, etc. Furthermore, it appears that the "co-impregnated" and "co-precipitated" catalysts are so different that their structure should be considered separately.

For a "co-impregnated" catalyst all, or the dominant fraction of, both Pt and Sn are located on the surface alumina support. For the following discussion they consider the role of only the support surface area, the metal concentration and the Sn/Pt ratio. First consider the case of a series of catalysts with constant Pt loading but with variable Sn/Pt ratios.

Their view of the catalyst surface is schematically depicted in Figure C3. The indirect and direct characterization data for Pt indicates that it is present in a zero valence state. The Pt will therefore be distributed among Pt atoms, Pt clusters that are larger than one atom and Pt present as a Pt/Sn alloy. Thus, a description of the state of Pt in the Pt-Sn-alumina catalyst involves determining the fraction present in each of the three states. Furthermore, both of the direct methods for determining the Pt/Sn alloy composition, XRD and TEM, indicates that only the PtSn = 1:1 alloy is formed. Thus,

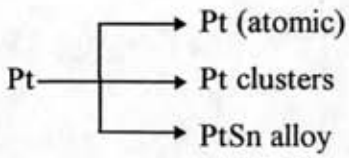

These three Pt states are represented schematically in Figure C3.

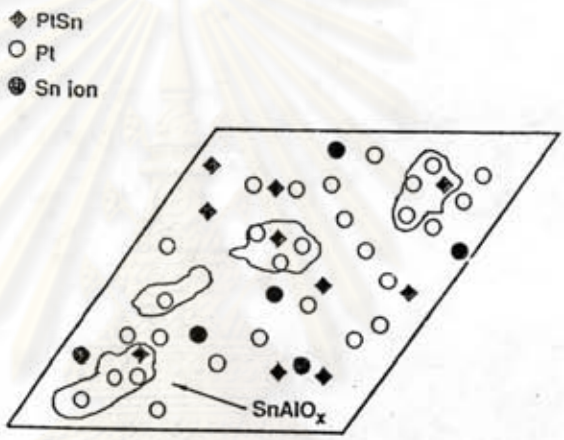

Figure C3. Schematic of proposed surface structure of a low (1:1) Pt/Sn alumina catalyst (Davis 1994).

The possible states of the tin are more numerous than for Pt. Many investigators believe they have presented strong evidence for the three stable valence states - Sn^{4+} , Sn^{2+} and Sn^0 - as well as for a host of compounds ranging from SnO_2 to metallic tin. It appears certain that the ratio of the oxidized to Sn^0 will vary with support surface area and Sn/Pt ratio. For a number of reasons we favor a "surface layer" of a tin compound that resembles tin aluminate, whether the oxidized tin is present as Sn^{2+} or Sn^{4+}. Even at 10 wt.% Sn on alumina, XRD does not detect any three dimensional tin compounds, including SnO_2. Furthermore, for most of the

techniques utilized to determine the chemical compounds containing tin would not be able to distinguish between the tin oxide and a corresponding tin aluminate.

Even if the tin does not actually form a species corresponding to a surface tin aluminate compounds, the oxidized tin is widely dispersed, the anion associated with it must be an oxide anion, or possibly a chloride ion if the catalyst still contains this element, and the oxidized tin interacts strongly with the alumina support. Thus, even if the tin is not present in a specific tin aluminate compound containing either Sn^{2+}or Sn^{4+}, the actual structure will resemble a tin aluminate widely dispersed over surface. Thus, we only consider two states for tin: a surface species for the oxidized tin that is or resembles a tin aluminate and Sn^0 that is essentially all presents as PtSn = 1:1 alloy. Thus,

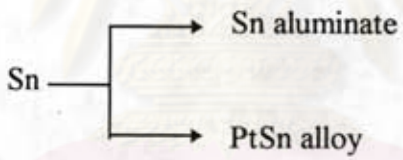

For the impregnated catalysts, the fraction of Pt presents as PtSn alloy increases with increasing Sn/Pt until, for a given Pt loading, further increases in Sn/Pt does not produce additional PtSn. The Sn/Pt ratio where the limiting amount of PtSn alloy occurs depends upon both Pt loading and surface area of the support. The lower the surface area, the smaller the Sn/Pt ratio that is needed to produce the limiting value. As the Pt loading is increased on a given support, the lower the Sn/Pt ratio needed to attain the limiting value.

APPENDIX D

DATA OF TPO EXPERIMENTS

Table D-1 Data of figure 5.2.

Time (min)	T(C)	CO2	CO2 /sec.	Integral area	Carbon(mg)	CO2/g -s	AreaCO2/g
0	50	0	0.0			0.00	
5	81	35	17.5	2625	1.050E-03	2938.41	440762
10	98	26	13.0	4575	1.830E-03	2182.82	768185
15	125	29	14.5	4125	1.650E-03	2434.68	692625
20	156	39	19.5	5100	2.040E-03	3274.23	856337
25	181	45	22.5	6300	2.520E-03	3777.96	1057828
30	205	53	26.5	7350	2.940E-03	4449.59	1234133
35	230	77	38.5	9750	3.900E-03	6464.50	1637115
40	255	116	58.0	14475	5.790E-03	9738.73	2430486
45	280	184	92.0	22500	9.000E-03	15447.65	3777957
50	305	292	146.0	35700	1.428E-02	24514.74	5994358
55	329	495	247.5	59025	2.361E-02	41557.53	9910840
60	358	1000	500.0	112125	4.485E-02	83954.60	18826818
65	380	1580	790.0	193500	7.740E-02	132648.26	32490429
70	405	2855	1427.5	332625	1.331E-01	239690.38	55850796
75	430	5818	2909.0	650475	2.602E-01	488447.85	109220733
80	457	12327	6163.5	1360875	5.444E-01	1034908.32	228503425
85	480	15156	7578.0	2061225	8.245E-01	1272415.88	346098630
90	505	14681	7340.5	2237775	8.951E-01	1232537.44	375742998
95	530	14725	7362.5	2205450	8.822E-01	1236231.45	370315333
100	557	16400	8200.0	2334375	9.338E-01	1376855.40	391963026
105	580	12955	6477.5	2201625	8.807E-01	1087631.81	369673081
110	605	201	100.5	986700	3.947E-01	16874.87	165676002
115	630	27	13.5	17100	6.840E-03	2266.77	2871247
120	655	35	17.5	4650	1.860E-03	2938.41	780778
125	680	62	31.0	7275	2.910E-03	5205.19	1221539
130	697	94	47.0	11700	4.680E-03	7891.73	1964538
			Total area =	1.489E+07		Total area =	2.50E+09
			Carbon (mg)=	5.9556	5.9556		
			%C =	6.62	6.62		

Table D-2 TPO data of 90 mg. coked Pt-Sn catalyst, 6 hr and 600°C propane reaction shown in figure 5.3

Time (min)	Temp.(C)	CO2 area	O2 area	CO2 area/sec	Integral area	Carbon(mg)
0	50	0	17480	0		
5	81	0	18505	0	0	0
10	103	25	17414	12.5	1875	7.50E-04
15	126	26	17499	13.0	3825	1.53E-03
20	157	34	17750	17.0	4500	1.80E-03
25	182	43	17380	21.5	5775	2.31E-03
30	206	55	17774	27.5	7350	2.94E-03
35	230	76	17456	38.0	9825	3.93E-03
40	256	125	17647	62.5	15075	6.03E-03
45	281	205	17290	102.5	24750	9.90E-03
50	305	346	16895	173.0	41325	1.65E-02
55	330	577	16156	288.5	69225	2.77E-02
60	358	1135	15551	567.5	128400	5.14E-02
65	382	1903	14918	951.5	227850	9.11E-02
70	405	3405	13541	1702.5	398100	1.59E-01
75	431	7075	10485	3537.5	786000	3.14E-01
80	458	14392	4638	7196.0	1610025	6.44E-01
85	482	16634	3635	8317.0	2326950	9.31E-01
90	506	17172	3635	8586.0	2535450	1.01E+00
95	531	17297	3634	8648.5	2585175	1.03E+00
100	558	17594	3655	8797.0	2616825	1.05E+00
105	580	17720	3653	8860.0	2648550	1.06E+00
110	606	17367	3698	8683.5	2631525	1.05E+00
115	631	16927	3840	8463.5	2572050	1.03E+00
120	657	12689	7373	6344.5	2221200	8.88E-01
125	680	28	17146	14.0	953775	3.82E-01
130	700	23	17138	11.5	3825	1.53E-03
				Total CO2 area =	**2.44E+07**	
				Carbon (mg) =	**9.7717**	**9.7717**
				%C =	**10.86**	**10.86**

Table D-3 TPO data of 35 mg. coked Pt-Sn catalyst, 6 hr and 600°C propane reaction shown in figure 5.3

Time (min)	Temp.(C)	CO2 area	O2 area	CO2 area/sec	Integral area	Carbon(mg)
0	50	0	14084	0.0		
5	80	11	14100	5.5	825	3.30E-04
10	99	15	14125	7.5	1950	7.80E-04
15	125	14	14111	7.0	2175	8.70E-04
20	156	15	14067	7.5	2175	8.70E-04
25	181	19	14047	9.5	2550	1.02E-03
30	205	26	13969	13.0	3375	1.35E-03
35	230	35	13917	17.5	4575	1.83E-03
40	255	54	13865	27.0	6675	2.67E-03
45	280	83	13803	41.5	10275	4.11E-03
50	304	133	13717	66.5	16200	6.48E-03
55	329	210	13595	105.0	25725	1.03E-02
60	358	392	13420	196.0	45150	1.81E-02
65	380	638	13142	319.0	77250	3.09E-02
70	405	1166	12676	583.0	135300	5.41E-02
75	430	2182	11768	1091.0	251100	1.00E-01
80	458	4888	9549	2444.0	530250	2.12E-01
85	480	8091	7167	4045.5	973425	3.89E-01
90	505	9724	6175	4862.0	1336125	5.34E-01
95	530	9811	6249	4905.5	1465125	5.86E-01
100	557	10976	5566	5488.0	1559025	6.24E-01
105	580	9005	7252	4502.5	1498575	5.99E-01
110	605	94	13840	47.0	682425	2.73E-01
115	630	46	13871	23.0	10500	4.20E-03
120	656	44	13868	22.0	6750	2.70E-03
125	680	39	13840	19.5	6225	2.49E-03
130	696	43	13819	21.5	6150	2.46E-03
				Total CO2 Area =	**8.66E+06**	
				Carbon (mg) =	**3.4640**	**3.4640**
				%C=	**9.90**	**9.90**

Table D-4 TPO data of 8.7mg coke from digestion shown in figures 5.4 and 5.5

Time (min)	T(C)	CO2	CO2 /sec.	Integral area	Carbon (mg)	CO2/g-s	AreaCO2/g
0	50	0	0		0	0.00	
5	80	0	0	0	0	0.00	0
10	98	0	0	0	0	0.00	0
15	125	12	6.0	900	0.0004	1641.09	246164
20	156	33	16.5	3375	0.0014	4513.01	923115
25	181	70	35.0	7725	0.0031	9573.04	2112907
30	205	151	75.5	16575	0.0066	20650.42	4533519
35	230	279	139.5	32250	0.0129	38155.41	8820875
40	255	410	205.0	51675	0.0207	56070.68	14133913
45	280	518	259.0	69600	0.0278	70840.51	19036678
50	304	583	291.5	82575	0.0330	79729.77	22585542
55	329	642	321.0	91875	0.0368	87798.47	25129236
60	358	740	370.0	103650	0.0415	101200.73	28349881
65	380	724	362.0	109800	0.0439	99012.61	30032001
70	405	899	449.5	121725	0.0487	122945.21	33293674
75	430	1200	600.0	157425	0.0630	164109.30	43058177
80	457	1803	901.5	225225	0.0901	246574.22	61602527
85	480	2680	1340.0	336225	0.1345	366510.76	91962747
90	505	4315	2157.5	524625	0.2099	590109.68	143493066
95	530	6485	3242.5	810000	0.3240	886873.99	221547551
100	557	8729	4364.5	1141050	0.4564	1193758.38	312094855
105	580	9767	4883.5	1387200	0.5549	1335712.92	379420694
110	605	10533	5266.5	1522500	0.6090	1440469.35	416427341
115	630	9069	4534.5	1470150	0.5881	1240256.01	402108804
120	656	1245	622.5	773550	0.3094	170263.40	211577911
125	680	34	17.0	95925	0.0384	4649.76	26236974
130	697	27	13.5	4575	0.0018	3692.46	1251333
			Total area =	**9140175**		**Total area=**	**2.50E+09**
			Carbon (mg) =	3.6561	3.6561		
			%C =	42.02	42.02		

Table D-5 TPO data of 5.1 mg coke from digestion shown in figures 5.4 and 5.5

Time (min)	T(C)	CO2	CO2 /sec	Integral area	Carbon(mg)	CO2/g-s	AreaCO2/g
0	50	0	0			0	
5	81	0	0	0	0	0	0
10	98	0	0	0	0	0	0
15	125	0	0	0	0	0	0
20	156	17	8.5	1275	5.10E-04	3944.68	591702
25	181	35	17.5	3900	1.56E-03	8121.40	1809913
30	206	75	37.5	8250	3.30E-03	17403.01	3828662
35	229	129	64.5	15300	6.12E-03	29933.17	7100427
40	256	228	114.0	26775	1.07E-02	52905.14	12425747
45	280	277	138.5	37875	1.52E-02	64275.11	17577037
50	304	325	162.5	45150	1.81E-02	75413.03	20953221
55	329	372	186.0	52275	2.09E-02	86318.92	24259792
60	358	442	221.0	61050	2.44E-02	102561.72	28332096
65	380	429	214.5	65325	2.61E-02	99545.20	30316039
70	404	524	262.0	71475	2.86E-02	121589.01	33170132
75	430	686	343.0	90750	3.63E-02	159179.51	42115278
80	457	1024	512.0	128250	5.13E-02	237609.06	59518285
85	480	1532	766.0	191700	7.67E-02	355485.43	88964173
90	504	2533	1266.5	304875	1.22E-01	587757.56	141486449
95	530	4135	2067.5	500100	2.00E-01	959485.80	232086505
100	557	6258	3129.0	779475	3.12E-01	1452106.92	361738908
105	579	7240	3620.0	1012350	4.05E-01	1679970.30	469811583
110	605	7638	3819.0	1115850	4.46E-01	1772322.26	517843883
115	630	1966	983.0	720300	2.88E-01	456190.83	334276963
120	656	24	12.0	149250	5.97E-02	5568.96	69263969
125	680	15	7.5	2925	1.17E-03	3480.60	1357435
130	697	20	10.0	2625	1.05E-03	4640.80	1218211
			Total area =	**5387100**		**Total area/g**	**2.50E+09**
			Carbon (mg)=	**2.1548**	**2.1548**		
			%C =	**42.25**	**42.25**		

Table D-6 TPO data of 2.9 mg coke from digestion shown in figures 5.4 and 5.5

Time (min)	T(C)	CO2	CO2 /sec.	Integral area	Carbon (mg)	CO2/g-s	AreaCO2/g
0	50	0	0			0	
5	80	0	0	0	0	0	0
10	98	0	0	0	0	0	0
15	124	0	0	0	0	0	0
20	156	15	7.5	1125	4.50E-04	4234.66	635198
25	180	30	15.0	3375	1.35E-03	8469.31	1905595
30	205	63	31.5	6975	2.79E-03	17785.56	3938230
35	229	113	56.5	13200	5.28E-03	31901.08	7452995
40	256	192	96.0	22875	9.15E-03	54203.60	12915702
45	280	236	118.0	32100	1.28E-02	66625.26	18124330
50	304	278	139.0	38550	1.54E-02	78482.30	21766134
55	329	321	160.5	44925	1.80E-02	90621.65	25365592
60	358	368	184.0	51675	2.07E-02	103890.24	29176783
65	380	364	182.0	54900	2.20E-02	102761.00	30997685
70	404	442	221.0	60450	2.42E-02	124781.21	34131331
75	429	578	289.0	76500	3.06E-02	163175.43	43193496
80	457	869	434.5	108525	4.34E-02	245327.76	61275479
85	480	1309	654.5	163350	6.53E-02	369544.35	92230817
90	504	2210	1105.0	263925	1.06E-01	623906.05	149017560
95	529	3723	1861.5	444975	1.78E-01	1051041.73	251242166
100	557	5615	2807.5	700350	2.80E-01	1585173.06	395432217
105	579	6420	3210.0	902625	3.61E-01	1812432.95	509640901
110	604	5562	2781.0	898650	3.59E-01	1570210.60	507396533
115	630	771	385.5	474975	1.90E-01	217661.34	268180792
120	655	18	9.0	59175	2.37E-02	5081.59	33411439
125	680	13	6.5	2325	9.30E-04	3670.04	1312743
130	697	17	8.5	2250	9.00E-04	4799.28	1270397
			Total area =	**4427775**		**Total area=**	**2.50E+09**
			Carbon (mg)=	**1.7711**	**1.7711**		
			%C =	**61.07**	**61.07**		

Table D-7 TPO data of 5 min. coked sample shown in figure 5.8

Time (min)	T(C)	CO2 area	CO2 area/g carbon	CO2 area/sec	Integral area	Carbon(mg)
0	50	0	0.00	0.00		
5	81	31	25203.25	15.50	2325	9.30E-04
10	98	20	16260.16	10.00	3825	1.53E-03
15	125	21	17073.17	10.50	3075	1.23E-03
20	156	12	9756.10	6.00	2475	9.90E-04
25	181	0	0.00	0.00	900	3.60E-04
30	205	17	13821.14	8.50	1275	5.10E-04
35	229	27	21951.22	13.50	3300	1.32E-03
40	256	50	40650.41	25.00	5775	2.31E-03
45	280	85	69105.69	42.50	10125	4.05E-03
50	304	149	121138.21	74.50	17550	7.02E-03
55	329	260	211382.11	130.00	30675	1.23E-02
60	358	451	366666.67	225.50	53325	2.13E-02
65	380	581	472357.72	290.50	77400	3.10E-02
70	405	878	713821.14	439.00	109425	4.38E-02
75	430	1215	987804.88	607.50	156975	6.28E-02
80	458	1887	1534146.34	943.50	232650	9.31E-02
85	480	2445	1987804.88	1222.50	324900	1.30E-01
90	505	2471	2008943.09	1235.50	368700	1.47E-01
95	530	360	292682.93	180.00	212325	8.49E-02
100	558	78	63414.63	39.00	32850	1.31E-02
105	580	26	21138.21	13.00	7800	3.12E-03
110	605	26	21138.21	13.00	3900	1.56E-03
115	631	11	8943.09	5.50	2775	1.11E-03
120	656	12	9756.10	6.00	1725	6.90E-04
125	680	15	12195.12	7.50	2025	8.10E-04
130	697	15	12195.12	7.50	2250	9.00E-04
				Total CO2 area =	**1670325**	
				Carbon(mg) =	**0.6681**	**0.66813**
				%C =	**0.74**	**0.74**

Table D-8 TPO data of 15 min. coked sample shown in figure 5.8

Time (min)	Temp.(C)	CO2 area	CO2 area/sec	Integral area	Carbon(mg)	CO2/g Carbon
0	50	0	0.0			0
5	82	16	8.0	1200	0.00048	11738.81
10	98	16	8.0	2400	0.00096	11738.81
15	125	15	7.5	2325	0.00093	11005.14
20	156	23	11.5	2850	0.00114	16874.54
25	182	16	8.0	2925	0.00117	11738.81
30	205	18	9.0	2550	0.00102	13206.16
35	230	33	16.5	3825	0.00153	24211.30
40	256	74	37.0	8025	0.00321	54292.00
45	281	99	49.5	12975	0.00519	72633.90
50	305	173	86.5	20400	0.00816	126925.90
55	330	289	144.5	34650	0.01386	212032.28
60	358	596	298.0	66375	0.02655	437270.73
65	380	870	435.0	109950	0.04398	638297.87
70	405	1432	716.0	172650	0.06906	1050623.62
75	430	2281	1140.5	278475	0.11139	1673514.31
80	458	3325	1662.5	420450	0.16818	2439471.75
85	481	4182	2091.0	563025	0.22521	3068231.84
90	505	5661	2830.5	738225	0.29529	4153338.22
95	531	3424	1712.0	681375	0.27255	2512105.65
100	558	116	58.0	265500	0.1062	85106.38
105	580	26	13.0	10650	0.00426	19075.57
110	606	17	8.5	3225	0.00129	12472.49
115	631	14	7.0	2325	0.00093	10271.46
120	657	0	0.0	1050	0.00042	0.00
125	681	0	0.0	0	0	0.00
130	697	0	0.0	0	0	0.00
			Total CO2 area =	**3.41E+06**		
			Carbon (mg) =	**1.3630**	**1.3630**	
			% C =	**1.51**	**1.51**	

Table D-9 TPO data of 40 min. coked sample shown in figure 5.8

Time (min)	T(C)	CO2	CO2 /sec	Integral area	Carbon (mg)	CO2/g-s	Area CO2/g
0	50	0	0.0			0	
5	80	13	6.5	975	0.00039	2.55E+03	3.83E+05
10	99	12	6.0	1875	0.00075	2.36E+03	7.37E+05
15	125	14	7.0	1950	0.00078	2.75E+03	7.66E+05
20	157	16	8.0	2250	0.0009	3.14E+03	8.84E+05
25	182	23	11.5	2925	0.00117	4.52E+03	1.15E+06
30	205	28	14.0	3825	0.00153	5.50E+03	1.50E+06
35	230	48	24.0	5700	0.00228	9.43E+03	2.24E+06
40	256	78	39.0	9450	0.00378	1.53E+04	3.71E+06
45	281	121	60.5	14925	0.00597	2.38E+04	5.87E+06
50	305	198	99.0	23925	0.00957	3.89E+04	9.40E+06
55	330	347	173.5	40875	0.01635	6.82E+04	1.61E+07
60	359	733	366.5	81000	0.0324	1.44E+05	3.18E+07
65	381	1173	586.5	142950	0.05718	2.30E+05	5.62E+07
70	405	2237	1118.5	255750	0.1023	4.40E+05	1.01E+08
75	430	4097	2048.5	475050	0.19002	8.05E+05	1.87E+08
80	458	6394	3197.0	786825	0.31473	1.26E+06	3.09E+08
85	481	6391	3195.5	958875	0.38355	1.26E+06	3.77E+08
90	505	7620	3810.0	1050825	0.42033	1.50E+06	4.13E+08
95	530	9264	4632.0	1266300	0.50652	1.82E+06	4.98E+08
100	558	3264	1632.0	939600	0.37584	6.41E+05	3.69E+08
105	580	178	89.0	258150	0.10326	3.50E+04	1.01E+08
110	606	48	24.0	16950	0.00678	9.43E+03	6.66E+06
115	631	32	16.0	6000	0.0024	6.29E+03	2.36E+06
120	657	33	16.5	4875	0.00195	6.48E+03	1.92E+06
125	680	30	15.0	4725	0.00189	5.90E+03	1.86E+06
130	697	33	16.5	4725	0.00189	6.48E+03	1.86E+06
			Total area =	**6361275**		**Total area=**	**2.50E+09**
			Carbon (mg)	**2.5445**	**2.5445**		
			%C	**2.83**	**2.83**		

APPENDIX D
DATA OF PORE SIZE DISTRIBUTION

Table E-1 Pore size distribution data of fresh Pt-Sn catalyst shown in figure 5.10

Fresh Pt-Sn catalyst #1		Fresh Pt-Sn catalyst #2		Sample 1		Sample 2	
Av. Pore Dia.(A)	dV/dlogD (cc./g-A)	Av.pore dia.(A)	dV/dlogD	log D	Volume(cc/g)	log D	Volume(cc/g)
20.1	0.220	20.3	0.238	1.303		1.307	
25.3	0.325	25.6	0.328	1.403	0.027	1.408	0.029
31.4	0.370	31.4	0.357	1.497	0.033	1.497	0.030
39.6	0.407	38.8	0.410	1.598	0.039	1.589	0.035
50.2	0.490	50.4	0.510	1.701	0.046	1.702	0.052
65.8	0.535	66.4	0.554	1.818	0.060	1.822	0.064
89.3	0.485	90.6	0.495	1.951	0.068	1.957	0.071
113.5	0.415	115.6	0.417	2.055	0.047	2.063	0.048
141.2	0.350	144.3	0.350	2.150	0.036	2.159	0.037
175.8	0.280	180.3	0.288	2.245	0.030	2.256	0.031
236.1	0.235	243.7	0.240	2.373	0.033	2.387	0.035
286.1	0.200	297.4	0.202	2.457	0.018	2.473	0.019
355.1	0.175	374.6	0.167	2.550	0.018	2.574	0.018
452.3	0.140	488.7	0.135	2.655	0.017	2.689	0.017
594.4	0.110	659.9	0.101	2.774	0.015	2.819	0.015
807.6	0.075	934.3	0.057	2.907	0.012	2.970	0.012
1183.5	0.050	1496.8	0.045	3.073	0.010	3.175	0.010
2034.2	0.049			3.308	0.012	**Total volume =**	**0.524**
				Total volume =	**0.521**		

Table E-2 Pore size distribution data of fresh Pt-Sn catalyst shown in figure 5.11

Av. Pore Dia.(A)	dV/dlogD (cc./g-A)	log D	Volume(cc/g)
20.1	0.220	1.303	
25.3	0.325	1.403	0.027
31.4	0.370	1.497	0.033
39.6	0.407	1.598	0.039
50.2	0.490	1.701	0.046
65.8	0.535	1.818	0.060
89.3	0.485	1.951	0.068
113.5	0.415	2.055	0.047
141.2	0.350	2.150	0.036
175.8	0.280	2.245	0.030
236.1	0.235	2.373	0.033
286.1	0.200	2.457	0.018
355.1	0.175	2.550	0.018
452.3	0.140	2.655	0.017
594.4	0.110	2.774	0.015
807.6	0.075	2.907	0.012
1183.5	0.050	3.073	0.010
2034.2	0.049	3.308	0.012
		Total volume =	**0.521**

Table E-3 Pore size distribution data of coked Pt-Sn catalyst
30 minutes propane reaction shown in figure 5.11

Average pore diameter(A)	dV/dlogD (cc./g-A)	log D	Volume(cc/g)
20.4	0.215	1.310	
25.7	0.312	1.410	0.026
31.5	0.350	1.498	0.029
38.8	0.399	1.589	0.034
49.6	0.500	1.695	0.048
67.6	0.533	1.830	0.069
89.5	0.495	1.952	0.063
110.3	0.430	2.043	0.042
138.5	0.355	2.141	0.039
178.5	0.288	2.252	0.035
234.7	0.244	2.371	0.032
306.8	0.195	2.487	0.026
406.9	0.149	2.609	0.021
559.0	0.110	2.747	0.018
828.0	0.072	2.918	0.016
1470.9	0.035	3.168	0.013
		Total volume=	**0.511**

Table E-4 Pore size distribution data of coked Pt-Sn catalyst
60 minutes propane reaction shown in figure 5.11

Av. pore dia.(A)	dV/dlogD (cc./g-A)	log D	Volume(cc/g)
20.6	0.200	1.314	
26.0	0.275	1.415	0.024
31.9	0.318	1.504	0.026
39.3	0.360	1.594	0.031
49.7	0.448	1.696	0.041
65.8	0.495	1.818	0.057
90.7	0.447	1.958	0.066
113.1	0.391	2.053	0.040
142.9	0.315	2.155	0.036
185.5	0.258	2.268	0.032
245.3	0.215	2.390	0.029
323.3	0.170	2.510	0.023
431.8	0.132	2.635	0.019
600.4	0.092	2.778	0.016
914.5	0.060	2.961	0.014
1644.4	0.025	3.216	0.011
		Total volume=	**0.465**

Table E-5 Pore size distribution data of coked Pt-Sn catalyst 180 minutes propane reaction shown in figure 5.11

Av. pore dia.(A)	dV/dlogD (cc./g-A)	log D	Volume(cc/g)
21.1	0.224	1.324	
26.5	0.275	1.423	0.025
32.5	0.299	1.512	0.025
39.8	0.360	1.600	0.029
50.7	0.450	1.705	0.043
69.1	0.476	1.839	0.062
91.1	0.440	1.960	0.055
112.4	0.380	2.051	0.037
141.1	0.318	2.150	0.034
181.5	0.261	2.259	0.032
238.2	0.218	2.377	0.028
311.6	0.175	2.494	0.023
412.8	0.142	2.616	0.019
565.4	0.100	2.752	0.017
840.7	0.065	2.925	0.014
1501.3	0.035	3.176	0.013
		Total volume=	**0.456**

Table E-6 Pore size distribution data of coked Pt-Sn catalyst 360 minutes propane reaction shown in figure 5.11

Av. pore dia.(A)	dV/dlogD (cc./g-A)	log D	Volume(cc/g)
21.9	0.240	1.340	
27.3	0.270	1.436	0.024
33.3	0.290	1.522	0.024
40.6	0.340	1.609	0.027
51.0	0.378	1.708	0.036
67.1	0.400	1.827	0.046
92.1	0.360	1.964	0.052
114.4	0.325	2.058	0.032
143.6	0.280	2.157	0.030
184.5	0.235	2.266	0.028
242.2	0.185	2.384	0.025
318.4	0.153	2.503	0.020
421.6	0.125	2.625	0.017
576.0	0.090	2.760	0.015
857.8	0.055	2.933	0.013
1576.3	0.030	3.198	0.011
		Total volume =	**0.400**

Table E-7 Pore size distribution of Pt-Sn catalyst treated in Ar at 600°C, 6 hr, shown in figure 5.12

Av.pore dia.(A)	dV/dlogD	log D	Volume (cc./g)
19.8	0.175	1.297	
25.2	0.290	1.401	0.024
31.0	0.366	1.491	0.030
38.2	0.408	1.582	0.035
49.0	0.500	1.690	0.049
66.9	0.566	1.825	0.072
90.2	0.520	1.955	0.070
116.3	0.448	2.066	0.053
140.9	0.366	2.149	0.034
178.9	0.300	2.253	0.035
233.6	0.250	2.368	0.032
305.4	0.200	2.485	0.026
403.9	0.160	2.606	0.022
550.9	0.116	2.741	0.019
784.7	0.080	2.895	0.015
1169.4	0.030	3.068	0.010
		Total volume =	**0.526**

VITA

Miss Nonglak Pinitniyom was born in Bangkok on April 14, 1973. She graduated high school from Wat Borwornmongkol School in 1990 and received her Bachelor of Engineering Degree in major of Chemical Engineering, from the Faculty of Engineering, King Mongkut's Institute of Technology Thonburi in 1994.